Simulation of electrostatic instabilities in a heliac configuration

E. Sánchez[1], I. Calvo[1], J. L. Velasco[1], R. Kleiber [2], R. Hatzky [3], M. Borchardt [2]

[1] *Laboratorio Nacional de Fusión, CIEMAT, 28040 Madrid, Spain*
[2] *Max Planck Institut für Plasmaphysik, D-17491, Greifswald, Germany*
[3] *Max Planck Institut für Plasmaphysik, D-85748, Garching, Germany*

Microinstabilities are supposed to be the cause of a large part of the transport in tokamak and stellarator plasmas. The appropriate framework to study these instabilities is the gyrokinetic formalism [1]. Much work has already been done in the study of electrostatic microinstabilities in tokamaks from the analytical and numerical points of view. In stellarators the lack of toroidal symmetry makes the problem more complicated and less progress has been made so far.

In this contribution we present global linear gyrokinetic simulations of electrostatic microinstabilities in the TJ-II heliac geometry carried out with the global, δf, particle-in-cell code EUTERPE [2, 3]. Recent upgrades in the code allow us to use fully kinetic electrons and ions and resolve spatial scales up to those typical from electron driven instabilities: trapped electron modes (TEM) and electron temperature gradient driven modes (ETG).

A linearized version of the Vlasov equation, $\frac{\partial \delta f_a}{\partial t} + \dot{\mathbf{R}}^0 \frac{\partial \delta f_a}{\partial \mathbf{R}} + \dot{v}_\parallel^{\,0} \frac{\partial \delta f_a}{\partial v_\parallel} = -\dot{\mathbf{R}}^1 \frac{\partial f_a^0}{\partial \mathbf{R}} - \dot{v}_\parallel^{\,1} \frac{\partial f_a^0}{\partial v_\parallel}$ is solved, where the equations of motion are:

$$\dot{\mathbf{R}} = \underbrace{v_\parallel \mathbf{b} + \frac{\mu B + v_\parallel^2}{B_a^* \Omega_a} \mathbf{b} \times \nabla \mathbf{B} + \frac{v_\parallel^2}{B_a^* \Omega_a} (\nabla \times \mathbf{B})_\perp - \frac{\nabla \phi_{ext} \times \mathbf{b}}{B_a^*}}_{\dot{\mathbf{R}}^0} \underbrace{- \frac{\nabla \langle \phi \rangle \times \mathbf{b}}{B_a^*}}_{\dot{\mathbf{R}}^1}$$

$$\dot{v}_\parallel = \underbrace{-\mu \left[\mathbf{b} + \frac{v_\parallel}{B_a^* \Omega_a} (\nabla \times \mathbf{B})_\perp \right] \nabla \mathbf{B}}_{\dot{v}_\parallel^{\,0}} \underbrace{- \frac{q_a}{m_a} \left[\mathbf{b} + \frac{v_\parallel}{B_a^* \Omega_a} (\mathbf{b} \times \nabla \mathbf{B} + (\nabla \times \mathbf{B})_\perp) \right] \nabla \langle \phi \rangle}_{\dot{v}_\parallel^{\,1}}$$

with $\dot{\mu} = 0$; q_a and m_a are the charge and mass respectively of the species a, $\Omega_a = \frac{q_a B}{m_a}$;and $B_a^* = B + \frac{m_a v_\parallel}{q_a} \mathbf{b} \cdot \nabla \times \mathbf{b}$. $\langle \phi \rangle$. ϕ_{ext} is the external equilibrium electric field, obatained in this case from Drift Kinetic Equation Solver (DKES) [4] calculations. A phase factor extraction is used in order to reduce the amount of resources required.

The kinetic equation is solved together with the quasineutrality (QN) equation, that in this work is used in three versions: when the electrons are considered adiabatic and the approximation $\Gamma_0(x) = e^{-x} I_0(x) \approx 1 - x$, valid for $x = k_\perp^2 \rho_i^2 << 1$, is considered, the QN reads $q_i \langle n_i \rangle - \frac{e n_0 (\phi - \bar{\phi})}{T_e} = -\nabla \frac{m_i n_0}{B^2} \nabla_\perp \phi$. I_0 is the modified Bessel function. For fully kinetic electrons, with the small k approximation, the QN can be written as $q_i \langle n_i \rangle - n_e = -\nabla \frac{m_i n_0}{B^2} \nabla_\perp \phi$. Finally, a Padé approximation $\Gamma_0(x) \approx 1/(1+x)$, that is valid for any scale, while maintaining a quadratic form for the operator acting on the potential, allows to write the QN equation as

$q_i\langle n_i\rangle - n_e = -\nabla\frac{m_i n_0}{B^2}\nabla_\perp\phi + \nabla\rho_i^2\nabla_\perp(q_i\langle n_i\rangle - n_e)$.

Preliminary simulations of ion temperature gradient (ITG) instabilities with the code EUTERPE in TJ-II configuration [5] allowed us to test the code in this geometry. In the present work, the threshold gradients for the ITG instability in TJ-II are studied in detail by means of simulations with adiabatic electrons and model density and temperature profiles. The simulations are carried out in the standard configuration with ion density and temperature profiles, defined as:

$$\frac{1}{T_i}\frac{dT_i}{ds} = -\kappa_T\left[\cosh^{-2}\left(\frac{s-s_0}{\Delta s_T}\right) - \cosh^{-2}\left(\frac{s_0}{\Delta s_T}\right)\right],$$
$$\frac{1}{n_i}\frac{dn_i}{ds} = -\kappa_n\left[\cosh^{-2}\left(\frac{s-s_0}{\Delta s_n}\right) - \cosh^{-2}\left(\frac{s_0}{\Delta s_n}\right)\right].$$

The electron density and temperature profiles are flat, with $T_e = T_i(s=s_0) = 100$ eV, $s_0 = 0.5$, $\Delta s_T = 0.2$, and $\Delta s_n = 0.42$; s being the normalized magnetic toroidal flux. From this profiles, the characteristic scale lengths at $s = s_0$ are $L_{Ti} = T_i/|\nabla T_i| \approx (0.97\kappa_T|\nabla T_i|)^{-1}$ and $L_n = n_i/|\nabla n_i| \approx (0.69\kappa_n|\nabla n_i|)^{-1}$, and the instability parameter $\eta_i = \frac{n_i|\nabla T_i|}{T_i|\nabla n|} \approx 1.4\kappa_T/\kappa_n$.

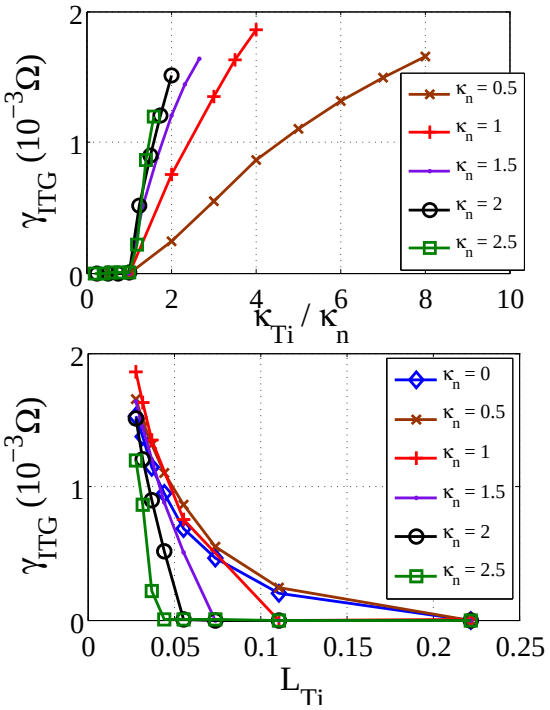

Figure 1: Growth rate of ITG modes vs κ_T/κ_n (top) and vs L_{Ti} (bottom). $\Omega \approx 0.95\cdot 10^8$ s^{-1}.

In these simulations a broad spectrum of unstable modes appear around $s = s_0$. In Fig. 1 the growth rate of the fastest growing mode is plotted versus the ratio κ_T/κ_n and L_{Ti}. A clear onset of the ITG instability is found for $\eta_i > \eta_{ith} \approx 1.4$. In the case that the density profile is flat the threshold L_n below which the modes are unstable is $L_{Tith} \approx .22$ m (see Fig. 1-bottom). The analysis of the wave-particle interaction shows that the parallel dynamics is stabilizing for these modes, which are destabilized mainly by the curvature and mirror contributions.

TJ-II has a great flexibility that allows to change the rotational transform (ι), magnetic well and plasma volume by changing the ratio of currents in the coils. The magnetic shear is usually very small, but using inductive current [6] introduces an extra knob to modify the rotational transform and the magnetic shear. Simulations in several magnetic configurations with different volume, magnetic well, rotational transform and magnetic shear have been carried out to study the influence of these parameters on the ITG stability.

The growth rate of ITG modes increases with the rotational transform while the magnetic shear has a slight stabilizing effect on these modes (see Fig. 2). No clear influence of the magnetic well or the fraction of trapped particles (mainly related to the plasma volume in TJ-II) has been found so far.

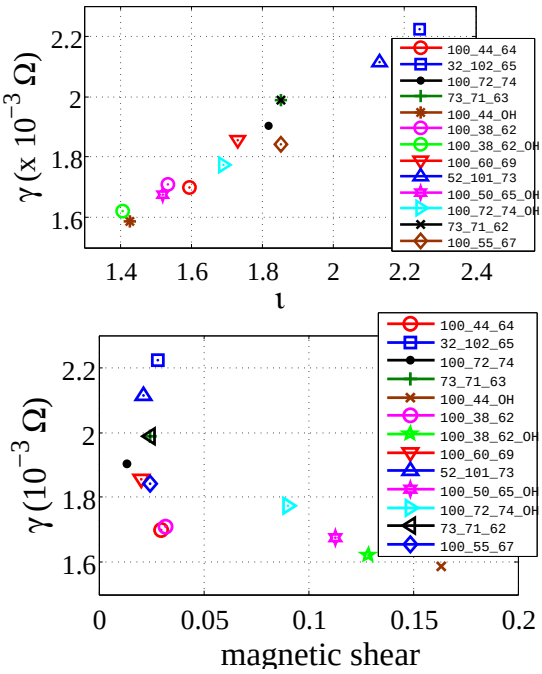

Figure 2: Growth rate of ITG modes vs ι (top) and magnetic shear (bottom). $\Omega \approx .95 \cdot 10^8$ s^{-1}.

Three plasma discharges representative of typical plasma regimes in TJ-II were selected: #18469 for ECRH heated plasmas, #28257 for NBI plasmas with bell-shaped density profile and #29211 for NBI dome-shaped plasmas. Their density and temperature profiles were reconstructed from experimental measurements using the Bayesian tools [7]. Based on the profiles characteristic lengths L_{Ti} and L_n no pure ITG instability is expected because temperature gradients do not exceed the threshold values (η_{ith} and L_{Tith}) obtained with model profiles. This expectation is confirmed by linear global gyrokinetic simulations using adiabatic electrons and the experimental profiles for these three plasma regimes: no instability is found in any case.

Simulations with fully kinetic ions and electrons have also been carried out using the density and temperature experimental profiles of discharge #18469 (ECRH) in the standard magnetic configuration. In these simulations unstable modes propagating in both the ion and electron diamagnetic directions appear. If the small k approximation is used, unstable modes in the range $75 < \mathrm{m} < 150$ (see Fig. 3) appear, corresponding to $0 < k\rho_i < 3$. The wavenumbers of these modes are in the range $1.25\ \mathrm{cm}^{-1} < \mathrm{k}_\theta < 22.5\ \mathrm{cm}^{-1}$. The maximum growth rate is $4.6 \cdot 10^{-5}$ s^{-1}. The unstable modes are mainly driven by trapped electrons, while the contribution of ions to the destabilization of the modes is much smaller, as shown by the analysis of wave-particle interaction. The parallel dynamics is stabilizing both for electrons and for ions.

When the neoclassical background electric field, obtained with DKES [4] using the experimental density and temperature profiles, is included in the simulation the maximum growth rate is slightly reduced (to $4.3 \cdot 10^5$ s^{-1}) and modes propagating in opposite directions are more clearly separated (see Fig. 3-(bottom)). In the outer region of the plasma $\rho > 0.7$ the modes propagate in the ion diamagnetic direction. In $0.4 < \rho < 0.6$ the modes propagate in the electron diamagnetic direction. Around $\rho = 0.6$, where the gradient of the NC electric field peaks,

the growth rate is reduced notably.

Simulations for the same ERCH plasma with kinetic electrons were run using a Padé approximant in the QN. In this case, unstable modes appear with much smaller scales, ranging from $0 < 75 < 2200$, which corresponds to $0 < k\rho_i < 10$. The most unstable modes are those with smaller scales and the growth rate reaches $\gamma_{max} \approx 9.6 \cdot 10^6$ s^{-1}. At moderate m values $m < 250$ the most unstable modes are loacated around $s \approx 0.45$ and the dominant drive is associated to the mirror term contribution of electrons, so that we can identify these modes with TEM. At larger m values, $250 < m < 2200$, the modes are located around $s \approx 0.35$ and the contribution associated to curvature is dominant, as would correspond to ETG modes.

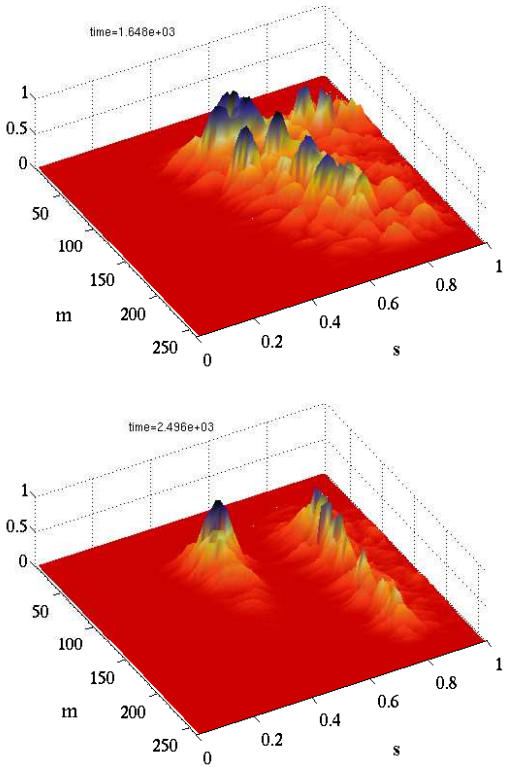

Figure 3: Mode amplitude in simulations with kinetic electrons and small k approximation, without (top) and with (bottom) electric field.

Only partial simulations with kinetic electrons have been carried out so far. Modes are suppressed using a squared Fourier filter. The small k approximation, when used, acts as an extra filter for the high m (k) modes. A huge amount of computational resources would be required in order to cover the full unstable spectrum in a simulation.

Acknowledgements

This work has been partially funded by the Ministerio de Economía y Competitividad of Spain under project and ENE2012-30832. The authors thank Antonio López-Fraguas for his help with VMEC calculations. The authors thankfully acknowledge the computer resources, technical expertise and assistance provided by the Barcelona Supercomputing Center-Centro Nacional de Supercomputación and the CIEMAT Computing Center.

References

[1] A. Brizard, T. S. Hahm, Rev. Modern Physics **2** 421-468 (2007).
[2] G. Jost, et. al., Phys. Plasmas **7** 1070664X (2001).
[3] V. Kornilov, et. al., Nucl. Fusion **45** 238-244 (2005).
[4] S. P. Hirshman, et. al. Phys. Fluids **29**(9) 2951-2959 (1986).
[5] E. Sánchez, et. al., 33rd Meeting of Royal Spanish Physics Society, Santander (2011).
[6] J. A. Romero, D. López-Bruna. Nucl. Fusion **43** (6) 387-392 (2003).
[7] B. P. van Milligen, et al. Rev. of Sci. Instruments **82** 073503 (2011).